Attribution of Responsibility for Short-Duration Voltage Variations in Power Distribution Systems via QGIS, OpenDSS, and Python Language

Arthur Gomes de Souza, Luiz Arthur Tarralo Passatuto, Wellington Maycon Santos Bernardes, Luiz Carlos Gomes Freitas, and Ênio Costa Resende

***Abstract*— Short-Duration Voltage Variations (SDVVs) are phenomena that significantly impact power quality. Although they typically last no longer than three minutes, such events can disrupt load operations and cause substantial production losses. This study presents an enhanced methodology for determining whether an SDVV event originates upstream or downstream of the point of common coupling between two agents interconnected through a transformer. Building upon the work of *Ferreira et al.*, whose original approach was applied to a circuit using *MATLAB/Simulink*, this research advances the methodology by applying it to both real and benchmark distribution systems using open-source tools, namely *QGIS*, *OpenDSS*, and *Python*™. The well-known IEEE 34-Bus Test System has been used to verify the methodology's generalizability. The method was also further validated through tests conducted on two actual Brazilian distribution feeders in Uberlândia, Minas Gerais: one supplying large industrial consumers such as a rice mill and a carbonated beverages factory, and the other serving a municipal wastewater treatment plant and a large photovoltaic plant. By using real, detailed and georeferenced data, the approach ensures an accurate representation of both the network topology and the installed equipment. The results confirm that the proposed methodology reliably identifies the origin of SDVV events. A key contribution of this study is that the attribution of responsibility remains robust regardless of variations in transformer winding configurations, fault resistance, circuit topology, load characteristics, or the presence of distributed generation. These findings demonstrate the accessibility, robustness and practical applicability, offering a valuable tool for utilities and researchers aiming to enhance power quality and accountability in distribution networks.**

***Index Terms*—OpenDSS, phenomenon responsibility, power quality, QGIS, short-duration voltage variation (SDVV).**

NOMENCLATURE

ANEEL	Brazilian Electricity Regulatory Agency.
ANN	Artificial Neural Networks.
BDGD	Geographic Database of the Distribution Company.
CLVR	Critical Load Voltage Regulator.
DG	Distributed Generation.
DVR	Dynamic Voltage Restorer.
FFT	Fast Fourier Transformer.
GIS	Geographic Information System.
HV	High Voltage.
LL	Line-to-Line.
LLL	Three-phase.
LLG	Double-Line-to-Ground.
LG	Single-Line-to-Ground.
MV	Medium Voltage.
PRODIST	Electric Power Distribution Procedures in the National Electric System.
SDVV	Short-Duration Voltage Variation.
STFT	Short-Time Fourier Transform.
UF	Unbalance Factor.

I. INTRODUCTION

A CONSUMER, whether an industry, a commercial company, or even a residential home, is exposed to challenges associated with the quality of electrical energy that may significantly impact their processes and operations [1], [2], [3]. One of these problems is the SDVV. According to the Brazilian Electricity Regulatory Agency (ANEEL) [4], SDVV refers to significant deviations in the voltage *rms* value, that occur in time intervals of less than three minutes. These phenomena are the main causes of power quality loss, caused by short circuits, switching of large loads that require high starting currents, or intermittent disconnection of cable within the electrical system. SDVVs are divided into voltage surges, voltage sags, and short interruptions, depending on the duration of the occurrence [5], [6].

Received 4 May 2025; revised 20 August 2025; accepted 31 August 2025. Date of publication 7 October 2025; date of current version 10 February 2026. Paper 2025-PSEC-0778.R1, presented at the 2024 International Workshop on Artificial Intelligence and Machine Learning for Energy Transformation (AIE), Vaasa, Finland, May 20–22, and approved for publication in the IEEE TRANSACTIONS ON INDUSTRY APPLICATIONS by the Power Systems Engineering Committee of the IEEE Industry Applications Society [DOI: 10.1109/AIE61866.2024.10561325]. This work was supported in part by Minas Gerais Research Funding Foundation (FAPEMIG) through Demanda Universal under Grant APQ-02176-22 and Grant APQ-04929-22, in part by Conselho Nacional de Desenvolvimento Científico e Tecnológico through CNPq under Grant 406881/2022-7, and in part by Coordenação de Aperfeiçoamento de Pessoal de Nível Superior - Brazil through CAPES - Finance Code 001, ROR: 00x0ma614. *(Corresponding author: Wellington Maycon Santos Bernardes.)*

Arthur Gomes de Souza, Luiz Arthur Tarralo Passatuto, Wellington Maycon Santos Bernardes, and Luiz Carlos Gomes Freitas are with the Department of Electric Power Systems (DEPSEE), Faculty of Electrical Engineering (FEELT), Federal University of Uberlândia (UFU), Uberlândia 38400-902, Brazil (e-mail: arthurgs@ufu.br; tarralo@ufu.br; wmsbernardes@ufu.br; lcgfreitas@ufu.br).

Ênio Costa Resende is with the Department of Electric Power Systems (DEPSEE), Faculty of Electrical Engineering (FEELT), Federal University of Uberlândia (UFU), Uberlândia 38400-902, Brazil, and also with the School of Technology and Innovations, Electrical Engineering, University of Vaasa, 65200 Vaasa, Finland (e-mail: eniocostaresende@ufu.br).

Color versions of one or more figures in this article are available at https://doi.org/10.1109/TIA.2025.3618601.

Digital Object Identifier 10.1109/TIA.2025.3618601

SDVV often lead to increased consumer complaints, malfunction or shutdown of sensitive equipment across residential, commercial, and industrial sectors. These disturbances may also interrupt production processes, cause economic losses, and compromise both facility and public safety [7], [8]. This article proposes a generalized methodology for accurately assigning responsibility in SDVV events, independent of the electrical system's specific configurations. The method is designed to be broadly applicable, enhancing the precision and reliability of disturbance source identification. The proposed approach enhances electrical network reliability and facilitates the integration of advanced analytical techniques. As a result, energy data can be managed more efficiently and interpreted with greater clarity.

Module 8 of Electric Power Distribution Procedures in the National Electric System (PRODIST) from Brazil evaluates the SDVVs, and these contingencies are stratified based on their duration and amplitude. After this stratification, the events are divided into nine sensitivity regions. The aim is to establish a correlation between the importance of each SDVV event and the sensitivity levels of the different loads connected to distribution systems, in Medium Voltage (MV) or High Voltage (HV). Next, the Unbalance Factor (UF) indicator is calculated, which characterizes the severity of the SDVV event [4].

It is important to highlight that the calculation of UF does not lead to any form of penalization or allocation of responsibility between the electricity companies and/or consumers. Instead, it merely assesses the event. Given the frequent occurrence of SDVV in power grids, a straightforward and practical method for attributing responsibility is essential. The startup of large motors may require mitigation strategies, such as the use of soft-start devices or pre-scheduled operations, to prevent voltage sags and ensure compliance with power quality standards. By defining clear responsibilities, this methodology facilitates efficient problem-solving and ensures the reliability of the grid.

Ferreira et al. [9] introduced a methodology for allocating responsibilities based on the analysis of voltage unbalances at the primary and secondary sides of the service transformer. Their original implementation was carried out using *MATLAB/Simulink*, a proprietary platform widely used for simulation in Electrical Engineering. Notably, their validation was performed using a simplified and fully controlled laboratory circuit, which limits its applicability to real-world conditions.

In contrast, the present study revisits and expands upon the original methodology by applying it to both real-world distribution feeders and a standardized IEEE benchmark circuit, using only open-source tools. This extension demonstrates the method's robustness and applicability in practical, large-scale scenarios. Particularly, the study proposes adaptations and improvements that enhance the applicability and scalability of the original method.

The revised methodology is initially tested on the test circuit from the reference [9], a simplified system used to validate foundational aspects. Following this, in sequence, it is applied to the IEEE 34-Bus System, a widely recognized benchmark for distribution network analysis. Subsequently, a more robust validation is conducted using two real feeders operated by *CEMIG Distribuição S/A* in the city of Uberlândia, Minas Gerais, Brazil. These feeders supply large industrial consumers and critical infrastructure, which are especially vulnerable to process disruptions caused by SDVV. The first feeder serves two major industrial facilities: a carbonated beverage factory and a rice processing plant. The second feeder supplies a municipal wastewater treatment plant and a large photovoltaic plant, underscoring the growing integration of distributed generation (DG), which has been rapidly expanding in Brazil and worldwide.

In addition, the network used for the simulations was obtained from the Geographic Database of the Distribution Company (BDGD), incorporating data on distribution lines (length, resistance, and reactance per kilometer), transformers, and loads, using *QGIS* [10] (previously known as Quantum Geographic Information System (GIS)). It is a full-featured, free and open source tool to perform different species of spatial analysis, allowing to create, edit, visualize, analyze and publish mapping information on Windows, Mac OS, Linux and others. Previously, it was challenging to find libraries that could automatically model feeders into files compatible with *OpenDSS*, and this process was done entirely manually. The analyzed feeders, *ULAE714* and *ULAU13*, were fully modeled based on the BDGD using BDGD2DSS[1], a custom *Python*™ library developed by two of the authors [11]. This tool converts data from the BDGD into files for simulation and analysis of electric distribution feeders in the *OpenDSS* environment. Alternatively, the modeling can also be performed using the library developed by *Radatz* et al. [12]. Once the complete network has been assembled, simulations were carried out in *OpenDSS*, and a *Python*™ routine was developed for processing.

It is well-known that *OpenDSS* is an open-source software widely used in both academic and commercial contexts to simulate electrical distribution networks [13], [14], [15]. Several research studies have used *OpenDSS* for various purposes, such as: (a) using chatbots to generate distribution network models, specifically for educational applications [16]; (b) optimizing with *MATLAB* the integration of Distributed Generation (DG) systems into the distribution network [17]; and (c) evaluation of the impact of the integration of charging stations for electric vehicles into a real network [18]. The versatility and widespread use of *OpenDSS* make it a valuable tool for energy system study. It also has an interface to *Python*™ via the *py-dss-interface* package [19] enabling seamless communication between script and software.

As is evident, a comprehensive explanation of the work's originality and specific contributions has been aforementioned to the reader. Other papers summarising the related studies are described in Table I. In general, these are studies that focus solely on the detection and measurement of SDVV, while others compare international reference standards. Only one study employs a methodology for the attribution of a SDVV, which served as reference for the present work.

Attention should be drawn to the fact that this article is an updated version of *Passatuto* et al. [1], enhancing the explanation

[1]Available in https://pypi.org/project/bdgd2dss/. The user should use the command 'pip install bdgd2dss' for package installation. Release on: July 31, 2025. The first commits found on Github are from September 2nd, 2024.

TABLE I
SUMMARY OF STUDIES ON SHORT-DURATION VOLTAGE VARIATION (SDVV)

Paper	Approach	Detection and Measurement	Attribution of Responsibility	Software in Use	Authors' Country
[5]	Uses Short-Time Fourier Transform (STFT) to analyze non-stationary SDVVs and Artificial Neural Networks (ANN) to identify five types of events. Simulations show STFT outperforms Fast Fourier Transformer (FFT) in detection accuracy, and ANN with a 10×10 hidden layer achieves 100% classification accuracy.	✓	×	-	Indonesia
[9]	Determines whether SDVVs originate upstream or downstream of a transformer's point of common coupling using unbalance indicator transfer. Computational and experimental studies validate the method, focusing solely on responsibility attribution without locating the disturbance.	×	✓	*MATLAB-Simulink®*	Brazil
[20]	Compares the proposed methodology existing in ANEEL procedures for classifying SDVVs with NRS 048 standard from South Africa, using real data from a Brazilian utility, and discusses benefits and limitations of each approach.	×	×	*Microsoft Excel®*	Brazil
[21]	Proposes a fast detection method for short-duration voltage variations in the grid to improve the response time of Dynamic Voltage Restorer (DVR), achieving delays under 1 ms even with voltage distortions, and validated through simulations and experiments.	✓	×	*MATLAB-Simulink®*	China
[22]	Evaluates three LED lamp models under transient conditions, analyzing their resilience to SDVV (sags) by varying magnitude, duration, and onset point, providing insights into their suitability for different applications.	×	×	-	Italy
[23]	Assesses the impact of SDVVs using Fuzzy Logic, based on the Brazilian index named Impact Factor, from a power quality regulation standard. Simulations demonstrated the method's ability to represent disturbance impacts considering uncertainties in magnitude and duration measurements.	×	×	*MATLAB-Simulink®*	Brazil
[24]	Uses discrete wavelet transform (Daubechies 4) with multiresolution analysis and different criteria (Shannon, log energy, and norm entropies) to classify SDVVs in distribution systems, demonstrated through *MATLAB*-based analysis.	×	×	*MATLAB-Simulink®*	India
[25]	Analyzes power quality disturbances (SDVV), specifically voltage transients, sags, swells, and interruptions, using continuous wavelet transform with Morlet wavelet in *MATLAB®*. The method enables quick identification of disturbance types via visualization of wavelet coefficients.	✓	×	*MATLAB-Simulink®*	India and Egypt
[26]	Detects and classifies SDVV (interruption, sag, swell) using Discrete Wavelet Transform for feature extraction and rule-based Fuzzy Logic for classification, validated through simulations.	✓	×	*MATLAB-Simulink®*	India
[27]	This work proposes a Monte Carlo–based method to estimate the Impact Factor of SDVV in distribution systems without extensive measurements. Validated on the IEEE 34-Bus System, it identifies critical regions, evaluates mitigation strategies, and supports utilities in reducing SDVV impacts.	✓	×	*OpenDSS*	Brazil
[28]	This paper presents an artificial intelligence-based methodology to assess power quality events, focusing on voltage transients and short-duration variations. It uses real and simulated data, infinite impulse response filtering, and machine learning classifiers.	✓	×	*MATLAB-Simulink® and Siemens PSS® E*	Lithuanian
[29]	This investigation analyzes the impact of neutral-grounding resistors on SDVVs in industrial power systems. By evaluating single-phase-to-ground and two-phase-to-ground faults, the study shows that grounding resistance mainly affects phase-to-ground voltages, with limited influence on phase-to-neutral or phase-to-phase voltages. The results provide guidance on optimal neutral grounding and load connections to minimize SDVV and equipment trips.	×	×	*ATP-EMTP*	Brazil and Sweden
[30]	Introduces a Critical Load Voltage Regulator (CLVR) that combines a DVR and an electric spring to protect critical loads from sags and long-term voltage fluctuations. Using fast thyristor switching, the CLVR is validated through simulations and experiments, showing improved performance over existing regulators.	✓	×	*PSCAD™/EMTDC™*	China

of methodology, as well as incorporating additional feeders with distinct characteristics and applying more computational simulations. While the previous study focused on an only single feeder, this work extends the analysis to the electrical circuit designed by *Ferreira* et al. [9], to the IEEE 34-Bus Test System, as well as two real feeders, *ULAE714* and *ULAU13*, providing a broader assessment of the proposed work across different network configurations.

The paper is divided as follows: Primarily, Section II discusses the methodology applied and explains the mathematical and computational tools used, as well as elucidates the acquisition and modeling of the electrical circuit with *OpenDSS* software and *Python*™ language. In Section III, the results are presented and critically analyzed. The validity of this investigation is corroborated through the testing of several aforementioned electrical networks. Finally, Section IV concludes the study and provides recommendations for future research.

II. METHODOLOGY

The SDVV events are *rms* voltage changes, namely interruption, swell, and sags. These phenomena represent momentary voltage variations in power systems: a sag is a temporary drop below a specified threshold, typically caused by short circuits or large load startups; a swell is a brief increase above the nominal level, often due to load switching or grounding issues; and an interruption occurs when the voltage falls below 5% of the reference value, indicating a near or total loss of supply. The duration is determined by the elapsed time interval in which the signal exceeds a certain threshold value [4], [31]. Most SDVV events are caused by short circuits [32].

According to *Furse* et al. [33], the most common causes of short circuits in power grids are: faulty equipment, human error, vehicle accidents, falling trees, strong winds, and storms. It is observed that most of these events are temporary, either due to the nature of the anomaly or due to protective measures, causing a voltage sag in the network.

According to *Bordalo* et al. [34] and *Martins* [35], the following average values for the short-circuits occurrence were determined by statistical analysis:

- Three-phase (LLL) short circuit: 3%;
- Double-Line-to-Ground (LLG) short circuit: 6%;
- Line-to-Line (LL) short circuit: 10% and

- Single-Line-to-Ground (LG) short circuit: 81%.

In other words, 97% of short circuits are asymmetric. Therefore, the analysis presented in this article to assign responsibility for SDVV is based on the propagation of UF between the primary and secondary sides of the transformer [9]. Unbalanced three-phase voltages and currents can be decomposed into their positive, negative, and zero sequence components, among other analysis techniques. The relationship between the original components A, B and C and the subsequent components is given by (1).

$$\begin{bmatrix} \dot{V}_a \\ \dot{V}_b \\ \dot{V}_c \end{bmatrix} \times \begin{bmatrix} 1 & 1 & 1 \\ 1 & a^2 & a \\ 1 & a & a^2 \end{bmatrix} = \begin{bmatrix} \dot{V}_{a_0} \\ \dot{V}_{a_1} \\ \dot{V}_{a_2} \end{bmatrix} \tag{1}$$

Once the sequence components of the voltages are obtained, the UF can be calculated using (2) and (3).

$$UF\%_{V_2} = \frac{V_{a_2}}{V_{a_1}} \times 100\% \tag{2}$$

$$UF\%_{V_0} = \frac{V_{a_0}}{V_{a_1}} \times 100\% \tag{3}$$

The methodology is based on the evaluation of the propagation behavior of negative sequence voltage unbalance in the transformer when a short circuit happens, and consequently a SDVV. For the evaluation, several short circuits were applied on the primary and secondary sides of the transformer, observing whether the type of fault influences the results. Another variation has been the type of connection of the primary and secondary windings.

The zero sequence UF will be not analyzed because this component may not be present depending on the type of connection, for example, if one of the windings is connected in a Δ design, making it impossible to use (3).

A further change, compared to the proposal of *Ferreira* et al. [9] is that the relationship between the UF, here denoted as UR_{PS}, of the primary and secondary sides is evaluated for the attribution of responsibility for the SDVV (4). The values on the primary and secondary sides are compared qualitatively in the reference, but no explicit factor or quantitative relationship between these values has been defined.

$$UR_{PS} = \frac{\text{UF}_{\text{primary}}}{\text{UF}_{\text{secundary}}} \tag{4}$$

This work proposes that in case of a short circuit occurs on the primary side of the substation, i.e. on the electric utility side, regardless of its type or the number of phases involved in the fault or the fault resistance value, the relationship defined by (4) will be $\geqslant 0.95$ (threshold) and the responsibility for the SDVV can be attributed to the electric utility. If, on the other hand, the fault occurs on the secondary side, i.e. on, the consumer side, the relationship defined by (4) is < 0.95, which means that the responsibility for SDVV lies with consumer connected to substation transformer.

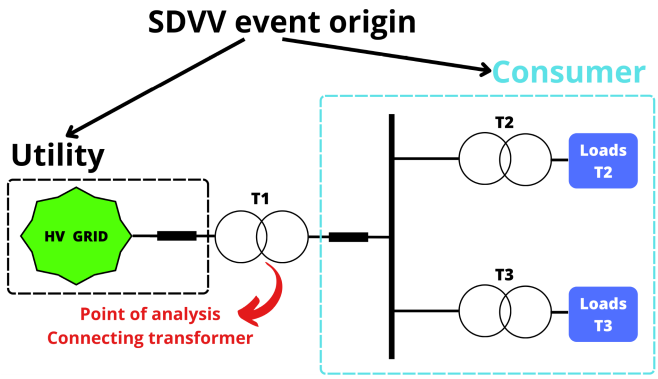

Fig. 1. Circuit from *Ferreira* et al. [9].

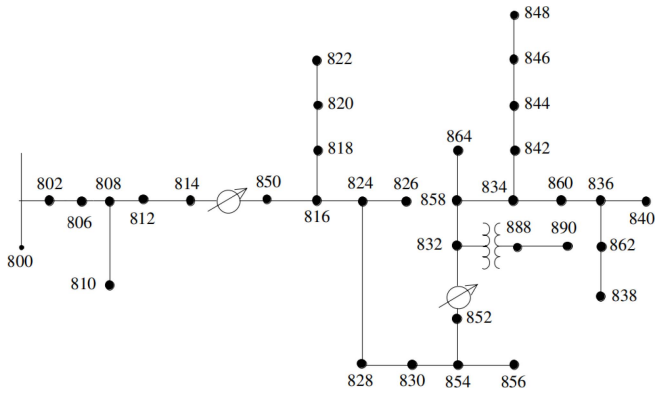

Fig. 2. IEEE 34-Bus System [39].

A. Case Studies

The test circuit from the [9] is considered in first. This benchmark system serves as a foundation for validating the proposed methodology. Following this, the study analyzes a benchmark power distribution system from IEEE, as well as two real distribution feeders, both located in the city of Uberlândia, Minas Gerais, Brazil. Each case presents distinct characteristics and contributes to a comprehensive evaluation of the proposed methodology. The analyzed systems are described as follows:

- **Circuit from *Ferreira* et al. [9]** – The test system used in *Ferreira* et al. [9] consists of a simple circuit with three transformers and two load groups, as shown in Fig. 1. The methodology proposed in this article will initially be tested on this electrical network, with Transformer 1 ($T1$) being the primary focus of the study.
- **IEEE 34-Bus System** – It models a 34-node, 24.9 kV medium-voltage radial distribution system with unbalanced loads and long, high-impedance lines, making it ideal for voltage drop and power loss studies. The system incorporates various load types, capacitor banks, and voltage regulators, providing a realistic representation of real-world distribution networks. Due to its complexity, it is extensively used in studies on voltage control, fault analysis, and the integration of distributed generation [36], [37], [38] (Fig. 2).

Fig. 3. Feeder *ULAE714* region. A rice mill and a carbonated drink industry in highlight [40].

- **Feeder *ULAE714*** – Originating from the Uberlândia 7 Substation, this 13.8 kV distribution circuit supplies electricity to consumers in the *Custódio Pereira* neighborhood. The feeder delivers power to both medium and low voltage consumers, encompassing residential areas, commercial establishments, and industrial facilities. Among the industrial loads connected to this feeder are a rice processing plant and a carbonated beverage factory, both of which contribute significantly to the feeder's demand due to their continuous and energy-intensive operations. Fig. 3 illustrates the layout and coverage of this feeder within the distribution network, highlighting the substation transformer and the loads of interest with their respective bus numbers (note that this numbering originates from the database in use).
- **Feeder *ULAU13*** – Originating from the Uberlândia 1 Substation, this 13.8 kV distribution circuit supplies electricity to consumers in the *Guarani* and *Tocantins* neighborhoods. It serves medium and low voltage loads, including residential, commercial, and institutional consumers. A key feature of this feeder is its connection to a large-scale photovoltaic farm, which contributes to the local distributed generation capacity. Additionally, the feeder supplies power to the municipal wastewater treatment plant, an essential infrastructure facility. Fig. 4 shows the layout and area of coverage of this feeder within the distribution system, highlighting the substation transformer and the loads of interest with their respective bus numbers (note that this numbering originates from the database used).

The test circuit from the [9], along with these feeders and the IEEE 34-Bus System, were selected to evaluate the proposed methodology in different operational scenarios, considering both industrial and infrastructure-critical loads, as well as a standardized benchmark for comparison.

This approach evaluates the methodology across different scenarios, considering load typology variations along the feeder. Both circuits were modeled using BDGD data, a public database with detailed electrical and geographical feeder information. These data are processed in *QGIS* following Module 10 of PRODIST, which standardizes Brazilian regulatory geographic information, ensuring consistency in network modeling [41], [42].

The BDGD contains comprehensive information about a vast region served by the utility, potentially covering an entire state. To simplify the studies, filters must be applied to delimit the analysis area. Fig. 3 illustrates feeder *ULAE714*, and Fig. 4 shows feeder *ULAU13*, both adding a layer with a visualization of the regions using the Google Satellite plug-in for *QGIS* [40].

In Figs. 3 and 4, the transmission lines responsible for supplying electrical power to the high-voltage substation are represented in pink. The green square indicates the substation, where the substation transformer is located and which will be the focus of this investigation for attributing responsibility, either upstream or downstream, while the white line represents the medium-voltage network. Regarding the points, red markers indicate distribution transformers, whereas yellow markers denote reclosers, which identify the connection points for consumers supplied by the medium-voltage network. Additionally, in Fig. 3,

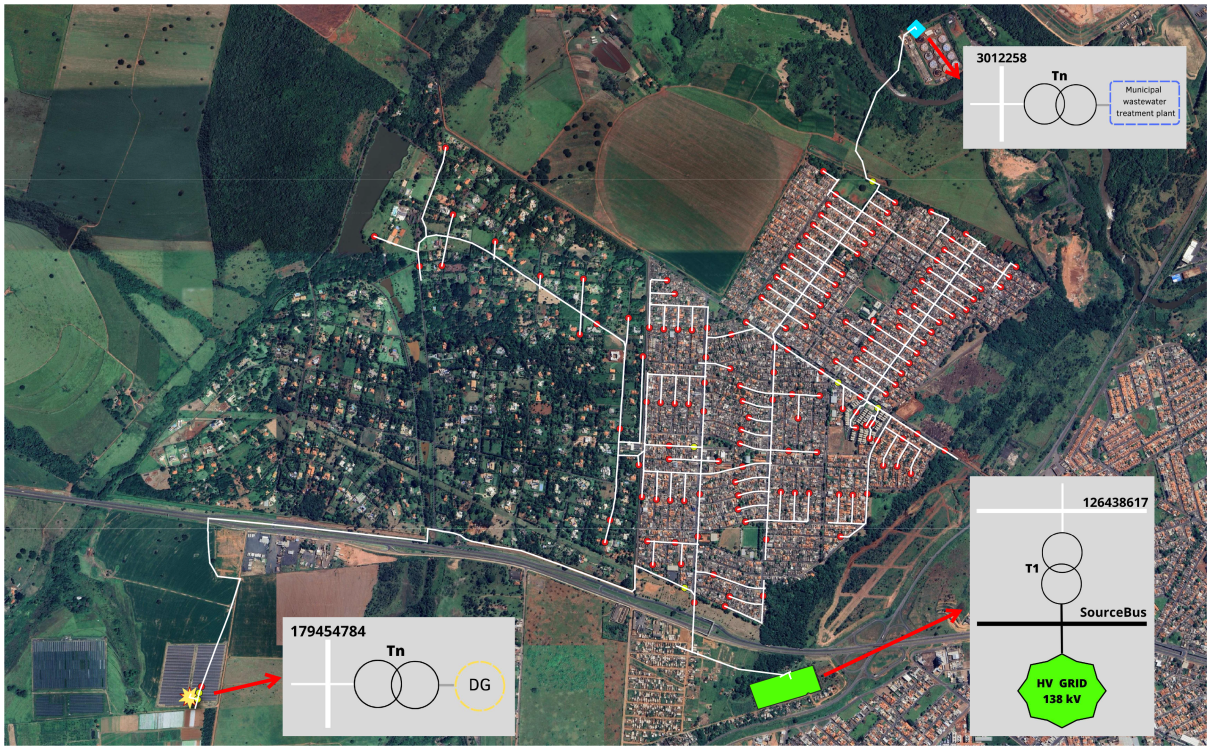

Fig. 4. Feeder ULAU 13 region. Photovoltaic farm and a municipal wastewater treatment plant in highlight [40].

the green diamond highlights the rice milling industry, while the black diamond represents the carbonated beverage industry. In Fig. 4, the yellow symbol marks the photovoltaic farm, and the blue diamond corresponds to the municipal wastewater treatment plant.

For the feeder modeling, the BDGD2DSS library, which is already publicly available [11], has been employed. A complete description of its design and functionalities will be presented in future works due to space constraints. This library processes the BDGD layers and converts them into . *dss* files, enabling the complete modeling of the system, including both medium- and low-voltage sections, as well as loads and distributed generation. The generated files can then be simulated within the *OpenDSS* environment. By automating data conversion, the library facilitates the integration of real-world network information into computational simulations, enhancing the accuracy of this analysis. The modeled feeders are in a public repository from *GitHub, Inc*© , available by the researchers in [43].

The BDGD layers used in the modeling can be grouped according to their function:

1) *Electrical Infrastructure:*
   - *SUB* – Substations of the system;
   - *CTMT* – Medium voltage circuits, used to identify the feeder;
   - *UNTRAT* – Substation transformers;
   - *UNTRMT* – Medium voltage transformers along the circuit.
2) *Electrical Network and Conductors:*
   - *SEGCON* – Detailed conductor data, including resistance and reactance.
   - *SSDMT*, *SSDBT*, and *RAMLIG* – Lengths of medium and low voltage segments, and connection branches.
3) *System Loads:*
   - *UCMT* and *UCBT* – Medium and low voltage consumer units, respectively, from which the load powers are extracted.
   - *PIP* – Public lighting points.
   - *CRVCRG* – Load curves associated with different types of consumers.
4) *Distributed Generation:*
   - *UGBT* and *UGMT* – Low and medium voltage generation units.
5) *Control and Protection Equipment:*
   - *UNSEMT* and *UNSEBT* – Medium and low voltage disconnect switches, essential to avoid improper interruptions in the modeling.
   - *EQRE* and *UNREMT* – Voltage regulators of the network.
   - *UNCRMT* – Capacitor banks used to correct the voltage level at certain feeder buses.

Thus, the developed model accurately represents the feeder's structure, ensuring that the simulation in *OpenDSS* properly reflects the electrical characteristics of the studied network. The modeling process followed the standard set by ANEEL [44], [45], [46]. The short-circuit level at the substation input was set to 100 MVA. The simulations were configured in daily mode, considering a 24-hour period.

The one-line diagram presented in Fig. 5 provides a simplified schematic representation of the feeders illustrated in Figs. 3 and 4. Transformer $T1$, which represents the one located at the

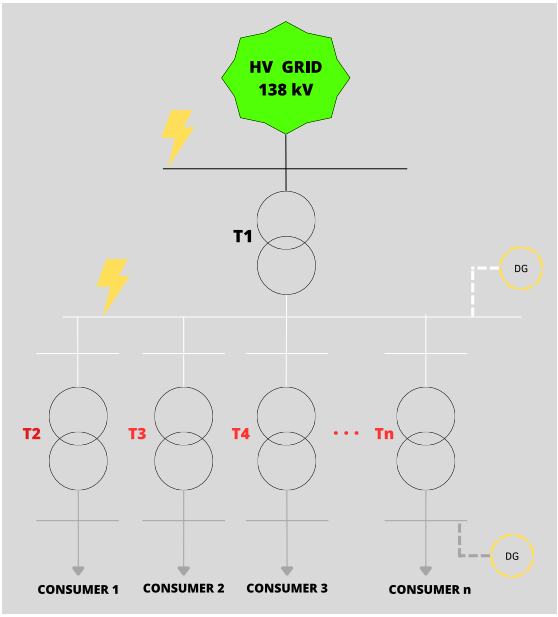

Fig. 5. Single-line diagram. Transformer $T1$ connection type will be changed interactively in the simulations (from $\Delta - Y_n$, to $Y_n - \Delta$, $\Delta - \Delta$ and $Y_n - Y_n$).

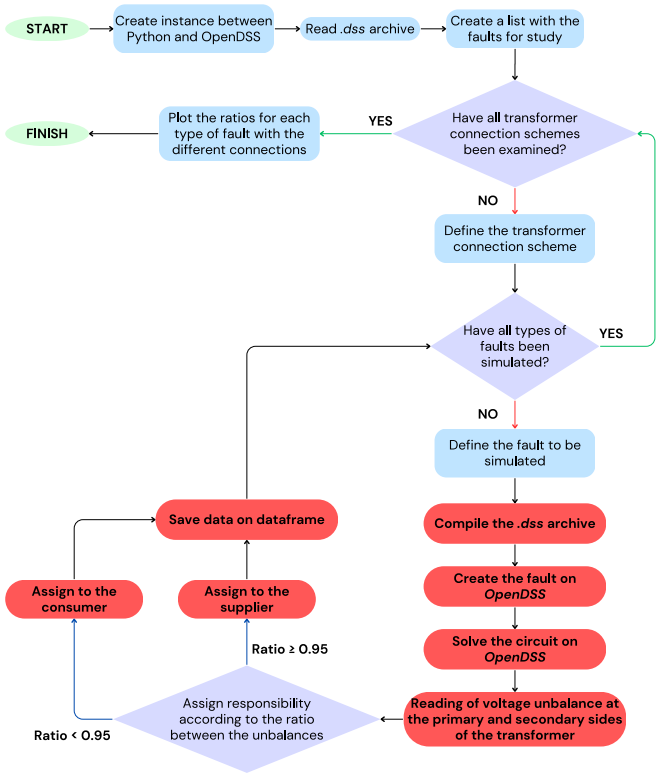

Fig. 6. Flowchart of the proposed intelligent algorithm.

substation, has its data extracted from the *UNTRAT* layer and will be the object of study in this analysis. Short-circuit tests are conducted on both the primary and secondary windings of this transformer, as illustrated in Fig. 5. During the simulation, the connection type will be adjusted accordingly in order to validate the proposed method and ensure accurate results for each configuration.

Transformers $T2$, $T3$, $T4$, and Tn represent the medium-voltage transformers from the *UNTRMT* layer, which may correspond to both the distribution network transformers and those of consumers supplied with medium voltage. Among these consumers, those in feeders *ULAE714* and *ULAU13*, highlighted in Figs. 3 and 4, are of particular importance. Information about these consumers is extracted from the *UCMT* and *UCBT* layers.

The white lines represent the medium-voltage circuit, with data extracted from the *SEGCON* and *SSDMT* layers, while the gray lines correspond to the low-voltage circuits from the *SSDBT* layer. Additionally, the presence of distributed generation (DG) is indicated at both medium and low voltage buses, reflecting its distribution along the circuit, as recorded in the *UGMT* and *UGBT* layers.

B. Computational Modeling and Analysis

To validate the proposed method, computational simulations of the electrical circuits have been performed using the *OpenDSS* software, also utilizing an interface script written in the *Python*™ language [47] with the py-dss-interface library. This package was used to facilitate direct communication and easy manipulation and to allow the export of data to more suitable formats or the creation of diagrams as desired.

To better understand the simulation, a flowchart is shown in Fig. 6. Basically, an instance is created between *Python*™ and *OpenDSS* using the mentioned package, reading the . *dss* file with the data of the circuit under study. Within the same script, a list of the twenty four fault cases to be studied was created. The four connection schemes of the transformer are then run through, and the faults contained in the list of cases are simulated for each of these schemes.

After compiling the circuit file with py-dss-interface, the simulation is run in daily mode for one day, with short circuits applied at noon, when solar incidence and DG contribution are highest. The *Python*™ script is used to extract the data of interest. This includes the unbalances of the negative sequence voltages in relation to the positive sequence voltages, on the primary and secondary sides of the transformer (supplier and load, respectively), each one in percent. By calculating the ratio between these unbalances, the responsibility is assigned to one of the parties involved in the system. Subsequently, the data is organized in a data frame using *Pandas* library [48] for further analysis. In the end, when all connection schemes have been run through, the graphs are plotted using *matplotlib* [49] for better visualization by the user.

The proposed flowchart can be used for different types of analyses related to the assignment of responsibility when SDVV occurs. The electrical system can be modelled directly with the. dss file. Much of the extracted data have the default settings from *OpenDSS* itself, and this may be checked directly via the manual [50], following the same standard procedures in Brazil.

The proposed script simulates 24 different fault cases, considering up to four transformer connection schemes, based

on the most commonly used configurations in the ANEEL database [41] and the schemes available in *OpenDSS*. However, not all connection schemes are tested in every case. When all four transformer connections are considered, the total number of simulations reaches 96 (4 connection schemes $\times$ 24 fault cases).

For each fault type, i.e., LG, LLG, or LL, simulations are conducted with short-circuit resistances of 0 Ω, 5 Ω, 10 Ω, and 20 Ω. The inclusion of these resistance values ensures a more comprehensive analysis, preventing extreme variations in fault currents and aligning with numerical values used in [51].

It can be observed that the simulations in *OpenDSS* consider a common reference for all elements of the circuit. Therefore, the application of LG and LLG faults on the Δ transformer side, will occur in one of the phases and the ground.

III. Results and Discussions

The simulations provide the desired data, with the most relevant being the ratio UR_{PS} between the UF on the primary (supplier) and secondary (consumer) sides of Transformer $T1$ during the fault, as defined by (4). This ratio determines which side is responsible for the SDVV, validating the proposed methodology. Voltage plots are not presented since the studies are conducted in DSS, a frequency-domain simulation engine specifically designed for power distribution systems.

The tests were carried out on the circuit from [9], the IEEE 34-Bus System, and the feeders *ULAE714* and *ULAU13*. In the IEEE 34-Bus System, different transformer connection configurations were tested to assess their influence on the proposed methodology. For the first feeder, all possible configurations of the substation transformer (Transformer $T1$) were analyzed, applying various types of short circuits to both the primary and secondary sides of the transformer while considering different short-circuit resistance values, as previously described. For the second feeder, an additional analysis was conducted to evaluate the impact of distributed generation (DG) by comparing scenarios with and without its presence. This comparison aimed to determine whether the introduction of DG affects the methodology's effectiveness.

A. Case 1 - Circuit From [9]

Table II presents the single-phase voltages at both the primary and secondary sides of transformer T1 (Δ-Y_n), corresponding to buses B1 and B2 in the circuit. Five scenarios are considered:

1) Pre-fault single-phase voltages at buses B1 and B2;
2) Single-phase voltages during LG fault at bus B1 (primary side of the transformer) with $R_{\text{fault}} = 0\ \Omega$;
3) Single-phase voltages during LG fault at bus B2 (secondary side of the transformer) with $R_{\text{fault}} = 0\ \Omega$;
4) Single-phase voltages during LL fault at bus B1 (primary side) with $R_{\text{fault}} = 20\ \Omega$ and;
5) Single-phase voltages during LL fault at bus B2 (secondary side) with $R_{\text{fault}} = 20\ \Omega$.

From these values, the unbalanced three-phase system is decomposed into three balanced sequence components (positive, negative, and zero sequence) using (1). Subsequently, the unbalance factors for both the primary and secondary sides are determined using (2) and (3). Finally, (4) is applied to compute the ratio between the primary and secondary unbalance factors, enabling the assessment of unbalance propagation. It is important to note that Table II presents results only for the short-circuit conditions corresponding to cases 1, 5, 20 and 24 of Table III, due to limitation of space.

TABLE II
Pre-Fault and Fault Voltages and Angles for the Circuit in [9] (Transformer: Δ-Y_n)

Bus	V_1 (pu)	θ_1 (°)	V_2 (pu)	θ_2 (°)	V_3 (pu)	θ_3 (°)
Pre-fault						
B1	0.99859	-0.1	0.99859	-120.1	0.99859	119.9
B2	0.98381	-31.0	0.98381	-151.0	0.98381	89.0
LG fault ($R_{\text{fault}} = 0\ \Omega$) at B1						
B1	0.00018	-78.8	0.92604	-119.3	1.02580	116.0
B2	0.58358	-64.9	0.52690	-120.2	0.98397	89.0
LG fault ($R_{\text{fault}} = 0\ \Omega$) at B2						
B1	0.94110	1.3	0.99862	-120.1	0.95062	117.6
B2	0.00011	-102.6	0.96902	-149.5	0.96947	87.4
LL fault ($R_{\text{fault}} = 20\ \Omega$) at B1						
B1	1.0077	-1.5	0.98237	-121.3	0.99859	119.9
B2	0.99501	-31.6	0.97921	-152.7	0.97017	88.7
LL fault ($R_{\text{fault}} = 20\ \Omega$) at B2						
B1	0.99762	-0.4	0.99643	-120.2	1.0003	119.8
B2	0.99043	-33.2	0.95543	-152.4	0.98383	89.0

Building upon this initial analysis for the Δ-Y_n configuration, the study extends to evaluate transformer $T1$ under four different possible winding connections: Δ-Y_n, Δ-Δ, Y_n-Y_n, and Y_n-Δ. Additionally, different short-circuit resistances are applied to both the primary and secondary windings to assess their influence on system behavior. The results, presented in Table III, illustrate how variations in transformer connections and fault conditions impact the propagation of unbalances and voltage deviations within the network.

Analyzing Table III, there is minimal variation due to transformer winding configurations or the applied short-circuit resistance. This indicates that, in a smaller, simplified, and controlled circuit, such changes do not significantly affect the results.

As a final point, the same Table III shows that primary-side faults yield an unbalance ratio near 1, while secondary-side faults cause a significant drop below 0.95. According to Fig. 6, this threshold distinguishes responsibility attribution. These results confirm that the unbalance ratio reliably indicates whether voltage disturbance originates on the primary or secondary side.

B. Case 2 - IEEE 34-Bus System

Table IV presents the pre-fault and during-fault voltages for a LG short circuit, as well as for a LL fault applied to both the primary and secondary sides of the transformer (SourceBus and Bus 800), with a fault resistance of 20 Ω. As in the previous case, these single-phase voltage values are used to calculate the unbalance factors and analyze their propagation throughout the system. It is important to note that Table IV includes only cases 1, 5, 20 and 24 from Table V.

TABLE III
SIMULATION RESULTS FOR DIFFERENT CONNECTIONS T1 IN CIRCUIT FROM [9]

Case	Fault Type	$\mathbf{R_{Fault}}$ (Ω)	$\mathbf{UR}_{PS}$ (Δ-Y_n)	$\mathbf{UR}_{PS}$ (Y_n-Δ)	$\mathbf{UR}_{PS}$ (Δ-Δ)	$\mathbf{UR}_{PS}$ (Y_n-Y_n)
1	LG Primary	0	1.0003	1.0003	1.0003	1.0003
2	LG Primary	5	1.0005	1.0005	1.0005	1.0005
3	LG Primary	10	1.0005	1.0005	1.0005	1.0005
4	LG Primary	20	1.0005	1.0005	1.0005	1.0005
5	LG Secondary	0	0.0712	0.1043	0.1037	0.0723
6	LG Secondary	5	0.1023	0.1043	0.1037	0.1023
7	LG Secondary	10	0.1036	0.1043	0.1037	0.1036
8	LG Secondary	20	0.1041	0.1043	0.1037	0.1041
9	LLG Primary	0	1.0000	1.0000	1.0000	1.0000
10	LLG Primary	5	1.0005	1.0005	1.0005	1.0005
11	LLG Primary	10	1.0005	1.0005	1.0005	1.0005
12	LLG Primary	20	1.0005	1.0005	1.0005	1.0005
13	LLG Secondary	0	0.0363	0.0552	0.0552	0.0375
14	LLG Secondary	5	0.1002	0.1012	0.1012	0.1002
15	LLG Secondary	10	0.1026	0.1031	0.1031	0.1026
16	LLG Secondary	20	0.1036	0.1039	0.1039	0.1036
17	LL Primary	0	1.0000	1.0000	1.0000	1.0000
18	LL Primary	5	1.0006	1.0006	1.0005	1.0005
19	LL Primary	10	1.0005	1.0005	1.0005	1.0005
20	LL Primary	20	1.0005	1.0005	1.0005	1.0005
21	LL Secondary	0	0.0552	0.0552	0.0552	0.0552
22	LL Secondary	5	0.1012	0.1012	0.1012	0.1012
23	LL Secondary	10	0.1031	0.1031	0.1031	0.1031
24	LL Secondary	20	0.1039	0.1039	0.1039	0.1039

TABLE IV
PRE-FAULT AND FAULT VOLTAGES AND ANGLES FOR THE CASE IEEE 34-BUS SYSTEM (TRANSFORMER: Δ-Y_n)

Bus	V_1 (pu)	θ_1 (°)	V_2 (pu)	θ_2 (°)	V_3 (pu)	θ_3 (°)
Pre-fault						
SourceBus	1.05	30.0	1.05	-90.0	1.05	150.0
800	1.05	0.0	1.05	-120.0	1.05	120.0
826	1.0101	-123	0	0	0	0
848	1.0436	-3.4	1.0351	-124.5	1.0367	115.9
LG fault ($R_{\text{fault}} = 0\ \Omega$) at Source Bus						
SourceBus	4.63E-05	-41.6	1.8087	-119.8	1.8095	179.8
800	1.0447	-0.2	1.0443	-119.8	1.05	120.0
826	1.0102	-122.9	0	0	0	0
848	1.0426	-3.7	1.0352	-124.4	1.0368	116
LG fault ($R_{\text{fault}} = 0\ \Omega$) at 800						
SourceBus	0.74128	47.8	1.05	-90.0	0.70676	134.8
800	0.023002	-79.3	0.96686	-107.3	0.94066	107.8
826	0.96132	-111.4	0	0	0	0
848	0.034897	141.6	0.99296	-113.7	1.031	104.1
LL fault ($R_{\text{fault}} = 20\ \Omega$) at Source Bus						
SourceBus	1.0503	29.9	1.0492	-90.0	1.05	150
800	1.0504	0	1.0497	-120.1	1.0494	120
826	1.0098	-123	0	0	0	0
848	1.0434	-3.5	1.0348	-124.6	1.036	115.9
LL fault ($R_{\text{fault}} = 20\ \Omega$) at 800						
SourceBus	1.05	30	1.0499	-90.0	1.0501	150
800	1.0501	0	1.0498	-120	1.05	120
826	1.01	-123	0	0	0	0
848	1.0437	-3.5	1.0349	-124.6	1.0367	115.9

TABLE V
SIMULATION RESULTS FOR DIFFERENT FAULT TYPES CASE IEEE 34-BUS SYSTEM

Case	Fault Type	$\mathbf{R_{Fault}}$ (Ω)	$\mathbf{UR}_{PS}$ (Y_n-Y_n)	$\mathbf{UR}_{PS}$ (Δ-Y_n)
1	LG Primary	0	1.0000	0.9998
2	LG Primary	5	0.9987	0.9997
3	LG Primary	10	0.9982	0.9996
4	LG Primary	20	0.9974	0.9993
5	LG Secondary	0	0.5543	0.4255
6	LG Secondary	5	0.5558	0.5558
7	LG Secondary	10	0.5558	0.5558
8	LG Secondary	20	0.5558	0.5558
9	LLG Primary	0	1.0000	1.0000
10	LLG Primary	5	0.9995	1.0003
11	LLG Primary	10	0.9995	1.0006
12	LLG Primary	20	0.9993	1.0012
13	LLG Secondary	0	0.3848	0.2296
14	LLG Secondary	5	0.5558	0.5558
15	LLG Secondary	10	0.5558	0.5558
16	LLG Secondary	20	0.5558	0.5558
17	LL Primary	0	1.0000	1.0000
18	LL Primary	5	0.9999	1.0002
19	LL Primary	10	0.9998	1.0004
20	LL Primary	20	0.9997	1.0008
21	LL Secondary	0	0.3855	0.3855
22	LL Secondary	5	0.5558	0.5558
23	LL Secondary	10	0.5558	0.5558
24	LL Secondary	20	0.5558	0.5558

In the IEEE 34-Bus System, the propagation of unbalance was analyzed considering two different configurations for the supply transformer, originally connected in Δ-Y_n at bus 800 in Fig. 2. Initially, tests were conducted with the original configuration, and subsequently, the transformer connection was modified to Y_n-Y_n to assess the impact of this change on the propagation of unbalance throughout the system. The results obtained for both configurations are presented in Table V, highlighting the

TABLE VI
PRE-FAULT AND FAULT VOLTAGES AND ANGLES FOR THE *ULAE714* FEEDER (TRANSFORMER: Δ-Y_n)

Bus	V_1 (pu)	θ_1 (°)	V_2 (pu)	θ_2 (°)	V_3 (pu)	θ_3 (°)
Pre-fault						
SourceBus	1.0369	-1.4	1.0373	-121.4	1.0371	118.6
126355009	1.0376	-32.0	1.0378	-151.9	1.0382	88.0
150345630	1.0258	-33.8	1.0263	-153.8	1.0269	86.2
150347944	1.0255	-33.8	1.026	-153.8	1.0267	86.2
LG fault ($R_{\text{fault}} = 0\ \Omega$) at SourceBus						
SourceBus	5.45E-07	-75.0	1.0217	-122.1	1.0516	118.1
126355009	0.60719	-62.5	0.5902	-122.7	1.0359	87.9
150345630	0.59853	-64.4	0.58268	-124.7	1.0218	85.9
150347944	0.59838	-64.4	0.58254	-124.7	1.0215	85.9
LG fault ($R_{\text{fault}} = 0\ \Omega$) at 126355009						
SourceBus	0.65586	27.7	1.0370	-121.4	0.58136	94.0
126355009	5.13E-05	-109.9	0.94572	-133.8	0.89311	70.6
150345630	0.0046874	-134.5	0.93934	-135.7	0.87886	68.8
150347944	0.0047199	-134.7	0.93916	-135.7	0.87864	68.8
LL fault ($R_{\text{fault}} = 20\ \Omega$) at SourceBus						
SourceBus	0.60461	-58.3	0.43420	-65.8	1.0367	118.6
126355009	0.94780	-60.9	0.10563	139.1	0.84925	116.7
150345630	0.93641	-62.8	0.10388	137	0.83941	114.8
150347944	0.93618	-62.8	0.10385	137	0.83921	114.8
LL fault ($R_{\text{fault}} = 20\ \Omega$) at 126355009						
SourceBus	1.00280	-6.4	0.98925	-121.7	1.0658	116.6
126355009	1.06360	-38.1	0.95195	-156.4	1.0371	88.0
150345630	1.0521	-39.9	0.94085	-158.4	1.0247	86.2
150347944	1.0519	-40	0.94063	-158.4	1.0245	86.2

variations in voltages and unbalances recorded at different points in the electrical network.

Analyzing the results in Table V, it is clear that for faults on the primary side, the UR$_{PS}$ values remain close to 1in both transformer configurations. The greatest variation occurs in case 12. In this scenario, the UR$_{PS}$ value changes from 0.9993 in the Y_n-Y_n configuration to 1.0012 in the Δ-Y_n configuration.

The absolute difference between these values is 0.0019, while the relative difference, considering the Y_n-Y_n configuration as a reference, is approximately 0.19%. This indicates that the impact of the transformer connection on the fault response on the primary side is minimal, with variations that are practically negligible in most practical applications.

On the other hands, for faults on the secondary side, it is observed that the unbalance ratio does not remain close to 1, indicating that the unbalance does not propagate in the same way as when the fault occurs on the primary side. As $ratio < 0.95$, the responsibility is assigned to the consumer according to Fig. 6.

Therefore, these outcomes support the methodology's premise that, when the SDVV occurs on the primary side, the unbalance ratio between the primary and secondary is close to 1. And it will be otherwise, in case the SDVV occurs on the secondary side.

C. *Case 3 - Feeder* ULAE714

Table VI presents the pre-fault and during-fault voltages for a LG short circuit, as well as for a line-to-line fault with a fault resistance of 20 Ω applied to both primary and secondary sides of the transformer (SourceBus and Bus 126355009). Repeating the previous process, these single-phase voltage values are used to calculate the unbalance factors and analyze their propagation throughout the system. It is important to note that Table VI includes only cases 1, 5, 20 and 24 from Table VII.

Table VII presents the simulation results for the four transformer connection schemes: Δ-Y_n, Y_n-Δ, Δ-Δ, and Y_n-Y_n. The results include different short circuit resistance values and the UR_{PS} ratios obtained for each configuration. It is observed that the variation in resistance has little influence on the UR_{PS} ratio when comparing cases with the same transformer and fault type. The most significant difference occurs in the Δ-Y_n connection for an LG fault on the secondary side (cases 5 and 6), showing an absolute variation of 0.1202. However, this variation does not significantly impact the overall analysis, as the UR_{PS} ratio remains far from unity in all cases.

When comparing different connection schemes, the results remain consistent across configurations. Even with variations in transformer connection, the UR_{PS} ratio stays close to unity when the fault occurs on the primary side. The largest observed difference appears in an LG fault on the secondary side, considering a fault resistance of 0 Ω, for the Δ-Y_n and Δ-Δ connections, resulting in a value of 0.2442. However, this difference does not affect the final conclusions, as the UR_{PS} ratio remains far from unity, reinforcing the robustness of the proposed methodology.

Thus, the study concludes that, in these cases, the UR_{PS} ratio is minimally influenced by the type of transformer winding connection, regardless of the presence or absence of a nonzero fault resistance. This finding is crucial for the assignment of responsibility in the occurrence of a SDVV, as the UR_{PS} ratio provides an objective criterion: when it exceeds a defined threshold, the fault is attributed to the primary side of the transformer (supplier). Given that the lowest observed value was 0.9985 and the highest was 1.0006, the established threshold of 0.95, as defined in the script according to Fig. 6, proves to be not only appropriate but could potentially be set even more restrictively, reinforcing the robustness of the methodology.

It is important to highlight that when a fault occurs on the secondary side, where the consumer is connected, the measurement of the UF at this location has minimal influence on the observed value at the primary side. Conversely, when the fault occurs on the primary side, the resulting unbalance directly impacts the UF on both sides, causing their values to become nearly identical.

D. *Case 4 - Feeder* ULAU13

Table VIII presents the pre-fault and during-fault voltages for a LG short circuit, as well as for a LL fault with a fault resistance of 20 Ω, applied to both primary and secondary sides of the transformer (SourceBus and Bus 126438617). Additionally, Table VIII shows the voltage behavior at the bus (179454784) of the photovoltaic farm. Following the same procedure as before, these voltages serve as the basis for calculating unbalance indicators and analyzing their propagation throughout the system. Note that only cases 1, 5, 20, and 24 from Table IX are included in Table VIII.

Observe that Table IX presents the values of the unbalance ratio UR_{PS} for the feeder, considering scenarios with and

TABLE VII
SIMULATION RESULTS FOR DIFFERENT CONNECTIONS FEDDER *ULAE714*

Case	Fault Type	$\mathbf{R_{Fault}}$ (Ω)	$\mathbf{UR}_{PS}$ (Δ-Y_n)	$\mathbf{UR}_{PS}$ (Y_n-Δ)	$\mathbf{UR}_{PS}$ (Δ-Δ)	$\mathbf{UR}_{PS}$ (Y_n-Y_n)
1	LG Primary	0	1.0003	1.0002	0.9997	0.9997
2	LG Primary	5	1.0004	1.0003	0.9993	0.9993
3	LG Primary	10	1.0005	1.0003	0.9990	0.9990
4	LG Primary	20	1.0006	1.0005	0.9985	0.9985
5	LG Secondary	0	0.5868	0.7171	0.7171	0.6278
6	LG Secondary	5	0.707	0.7171	0.7171	0.7049
7	LG Secondary	10	0.7138	0.7171	0.7171	0.7130
8	LG Secondary	20	0.7159	0.7171	0.7171	0.7157
9	LLG Primary	0	1.0000	1.0001	1.0001	1.0001
10	LLG Primary	5	1.0001	1.0000	1.0001	1.0001
11	LLG Primary	10	1.0001	1.0000	1.0001	1.0001
12	LLG Primary	20	1.0001	1.0000	1.0001	1.0001
13	LLG Secondary	0	0.3137	0.5579	0.5579	0.4566
14	LLG Secondary	5	0.7018	0.7001	0.7001	0.6981
15	LLG Secondary	10	0.7118	0.7114	0.7114	0.7108
16	LLG Secondary	20	0.7151	0.7152	0.7152	0.7148
17	LL Primary	0	1.0007	1.0007	1.0002	1.0002
18	LL Primary	5	1.0003	1.0003	1.0002	1.0002
19	LL Primary	10	1.0005	1.0005	1.0002	1.0002
20	LL Primary	20	1.0006	1.0006	1.0004	1.0004
21	LL Secondary	0	0.5579	0.5579	0.5579	0.5579
22	LL Secondary	5	0.7001	0.7001	0.7001	0.7001
23	LL Secondary	10	0.7114	0.7114	0.7114	0.7114
24	LL Secondary	20	0.7152	0.7152	0.7152	0.7152

TABLE VIII
PRE-FAULT AND FAULT VOLTAGES AND ANGLES FOR THE *ULAU13* FEEDER (TRANSFORMER: Δ-Y_n)

Bus	V_1 (pu)	θ_1 (°)	V_2 (pu)	θ_2 (°)	V_3 (pu)	θ_3 (°)
Pre-fault						
SourceBus	1.042	0.5	1.0407	-119.5	1.0403	120.5
126438617	1.0412	-29.2	1.0418	-149.3	1.0393	90.7
179454784	1.0426	-29.1	1.0431	-149.2	1.0403	90.8
3012258	1.0398	-59.1	1.0429	-179.2	1.0401	60.7
LG fault ($R_{\text{fault}} = 0\ \Omega$) at SourceBus						
SourceBus	5.46E-07	-74.3	1.0157	-120.3	1.0663	119.7
126438617	0.61515	-60	0.58661	-120.1	1.0406	90.7
179454784	0.61584	-59.9	0.58759	-119.9	1.042	90.9
3012258	0.92679	-78.4	0.34761	177.8	0.90848	79.8
LG fault ($R_{\text{fault}} = 0\ \Omega$) at 126438617						
SourceBus	0.6467	29.6	1.0421	-118.9	0.59592	95.7
126438617	5.13E-05	-109.5	0.93897	-130.4	0.90692	74
179454784	0.000599	53.9	0.94007	-130.2	0.90912	74.2
3012258	0.5248	-105.7	0.54327	-130	1.0441	62
LL fault ($R_{\text{fault}} = 20\ \Omega$) at SourceBus						
SourceBus	0.6087	-56.3	0.43468	-62.9	1.0417	121.0
126438617	0.95217	-57.6	0.10649	140.3	0.85154	120.2
179454784	0.95381	-57.4	0.10687	140.7	0.85292	120.4
3012258	1.0428	-58.3	0.60983	124.5	0.43482	117.7
LL fault ($R_{\text{fault}} = 20\ \Omega$) at 126438617						
SourceBus	1.0088	-4.4	0.99748	-119.7	1.0726	118.4
126438617	1.0677	-35.4	0.95816	-153.5	1.0457	90.7
179454784	1.0683	-35.2	0.95953	-153.3	1.0476	90.9
3012258	1.0877	-61.9	1.0027	174	0.98281	60.4

without DG, as well as variations in the transformer winding connection (Δ-Y_n and Y_n-Y_n) and short circuit resistance.

The analysis of Table IX confirms that both the variation in short circuit resistance and the configuration of the transformer windings do not significantly influence the unbalance ratios, as observed in Case 1 and 2, leading to the same decisions.

Furthermore, when comparing the results with and without the presence of DG, the largest absolute difference observed was 0.0021 for the Δ-Y_n connection in a line-to-line fault on the primary side with $R_{Fault} = 0\ \Omega$, corresponding to a relative variation of approximately 0.21%. This minimal impact confirms that the presence of DG has a negligible effect on the UR_{PS} ratios and, consequently, does not influence the assignment of responsibility in a SDVV.

It is again confirmed, in another feeder, that when the SDVV occurs on the transformer's primary side, the ratio UR_{PS} is close to a unit value, while this is not the case on the secondary side. Thus, if UR_{PS} is close to 1, the responsibility lies with the supplier; otherwise, the responsibility is with the consumer.

For better visualization, the script produces a scatter plot as presented in Fig. 7, showing the ratio between primary and secondary UF for each case considering the two connection schemes. The data used corresponds to the values presented in Table IX. To enhance interpretation, different markers are used to distinguish between faults occurring on the primary and secondary sides of the transformer. Visually, there is little difference between the points of the two connection cases. There is a noticeable distance between the cases where responsibility lies with the supplier and those one where the consumer is responsible. This observation further confirms the earlier finding regarding the minimal impact of the type of transformer connection. The threshold used for attribution is indicated in the figure and proves to be satisfactory for distinguishing between responsibilities.

TABLE IX
SIMULATION RESULTS FOR DIFFERENT CONNECTIONS FEDDER *ULAU13* WITH AND WITHOUT DGS

Case	Fault Type	R_{Fault} (Ω)	UR_{PS} (Y_n-Y_n) without DGs	UR_{PS} (Y_n-Y_n) with DGs	UR_{PS} (Δ-Y_n) without DGs	UR_{PS} (Δ-Y_n) with DGs
1	LG Primary	0	1.0001	0.9984	0.9996	1.0000
2	LG Primary	5	1.0000	0.9981	0.9996	1.0000
3	LG Primary	10	1.0000	0.9978	0.9995	1.0001
4	LG Primary	20	1.0000	0.9972	0.9995	1.0001
5	LG Secondary	0	0.6264	0.6265	0.5852	0.5855
6	LG Secondary	5	0.7031	0.7036	0.7052	0.7058
7	LG Secondary	10	0.7113	0.7117	0.7121	0.7125
8	LG Secondary	20	0.7142	0.7144	0.7144	0.7146
9	LLG Primary	0	0.9998	1.0003	0.9996	0.9996
10	LLG Primary	5	0.9998	1.0002	0.9996	0.9996
11	LLG Primary	10	0.9998	1.0001	0.9997	0.9996
12	LLG Primary	20	0.9997	0.9999	0.9997	0.9997
13	LLG Secondary	0	0.4555	0.4558	0.3132	0.3132
14	LLG Secondary	5	0.6966	0.6971	0.7002	0.7008
15	LLG Secondary	10	0.7091	0.7096	0.7101	0.7106
16	LLG Secondary	20	0.7133	0.7136	0.7135	0.7138
17	LL Primary	0	0.9997	0.9999	0.9996	1.0015
18	LL Primary	5	0.9997	0.9999	0.9996	1.0009
19	LL Primary	10	0.9997	0.9999	0.9996	1.0006
20	LL Primary	20	0.9997	1.0002	0.9996	1.0009
21	LL Secondary	0	0.5565	0.5568	0.5565	0.5568
22	LL Secondary	5	0.6987	0.6989	0.6987	0.6989
23	LL Secondary	10	0.7099	0.7102	0.7099	0.7102
24	LL Secondary	20	0.7136	0.7139	0.7136	0.7139

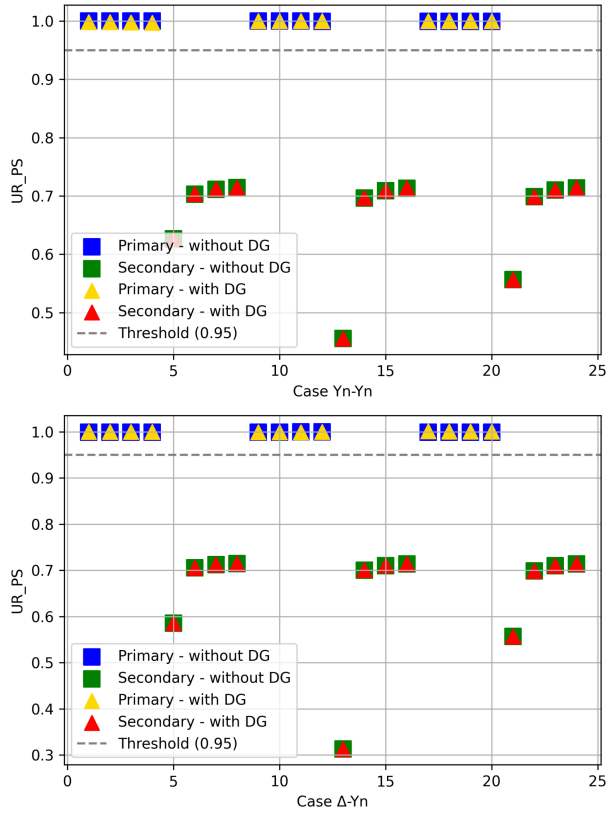

Fig. 7. Connection schemes with UF ratios between primary and secondary sides of transformer in cases of SDVV.

This study was conducted using a computer with the following specifications: an Intel(R) Core(TM) i5-8500 CPU @ 3.00 GHz processor, 8 GB of RAM, a 500 GB SSD, running Windows 10 Pro (version 22H2, 64-bit), with *Python*™ version 3.11.0 and installed *OpenDSS* version 9.6.1.3. The simulation time for feeder *ULAE714* was 793,33 seconds, while for feeder *ULAU13*, it was 1275,97 seconds. Meanwhile, the IEEE 34-Bus System simulation took less than 10 seconds.

IV. CONCLUSION

This paper demonstrates that the methodology proposed by *Ferreira* et al. [9], initially applied to simplified circuits, can also be successfully extended to complete and complex real distribution feeders. By implementing the approach in both actual utility networks and the IEEE 34-Bus Test System, this study confirms its applicability in more realistic and operationally relevant scenarios. The use of *OpenDSS*, combined with *Python*™, enhances the simulation and analysis process, while offering an accessible and open-source alternative to commercial tools. Additionally, the integration of real network data from the BDGD strengthens the practical value and reliability of the improved methodology.

This study contributes to the field of responsibility attribution for SDVV by analyzing various factors that may impact unbalance propagation, including transformer winding configurations, fault resistance variations, different circuit types with diverse load compositions, and the presence of DG. The results indicate that when the ratio between unbalance factors is below 0.95, the responsibility is attributed to the consumer side, highlighting this threshold as a key indicator. Conversely, values equal to or greater than 0.95 suggest that the disturbance originated on the supplier side. The analysis also revealed that regardless of minor variations introduced by transformer connections and fault resistances, the overall trend remained consistent. Furthermore, despite the rapid expansion of distributed

generation (DG) in modern distribution networks, the proposed methodology remains robust and unaffected. The evaluation of multiple circuit configurations with varying load conditions further confirms its reliability and adaptability.

It is important to note that this work does not aim to pinpoint the exact physical location of the event within the network or to numerically allocate responsibility for it, which is a limitation of the study and could be addressed in future research. Instead, its purpose is to determine whether the disturbance occurred upstream or downstream of the analysis point, providing a methodology for responsibility attribution.

Thus, the proposed methodology contributes to regulatory standards for events such as SDVV, relying on widely accessible software and real data from electric utilities. The data were obtained from a public repository. However, it should be emphasized that computational simulations may not fully reflect the current state of the grid, as the utility company frequently makes unannounced updates to the database.

One of the main challenges faced during the research was the accurate modeling of the circuit and the development of the simulation code using *Python*™. The first difficulty has been the limited availability of modeling tools, which was overcome through the use of a custom library developed by two of the authors and released to the public, available in [11]. This library will be described in detail in future works. The second challenge involved to create a script capable of simulating various types of faults, which was greatly facilitated by the *py-dss-interface* library [19]. Another significant difficulty was the potential presence of incorrect or incomplete information in the publicly available BDGD data, which required careful verification during the modeling process.

The current results offer significant contributions to the energy transformation sector, providing a method that combines computational analysis with relevant power system data to evaluate recurring power quality events in the electrical grid. Future work will aim to incorporate battery banks and additional consumers, refining the responsibility attribution to individual consumers or groups, rather than just identifying the responsible side. Additionally, future investigations involving Neural Networks [52], [53], [54], [55], [56], [57], [58] may be explored as a means to enhance classification accuracy and automate the attribution process, enabling more adaptive and intelligent analysis of complex power quality patterns in modern distribution networks. For this objective, computational techniques such as deep models, multilayer perceptrons, or radial basis functions may be used for training and validation. Moreover, future studies may also include sensitivity analyses and statistical evaluations to expand and validate the robustness of the results under varying grid conditions and parameter uncertainties.

Acknowledgment

The authors also thank the Programa de Pós-graduação em Engenharia Elétrica (PPGEELT) from the Federal University of Uberlândia (UFU).

References

[1] L. A. T. Passatuto, A. G. d. Souza, W. M. S. Bernardes, L. C. G. Freitas, and E. C. Resende, "Assignment of responsibility for short-duration voltage variation via QGIS, OpenDSS and python," in *Proc. Int. Workshop Artif. Intell. Mach. Learn. Energy Transformation*, 2024, pp. 1–6, doi: 10.1109/AIE61866.2024.10561325.

[2] Dino, "Falhas no fornecimento de energia prejudicam indústrias," 2023. Accessed: Sep. 6, 2025 (in Portuguese). [Online]. Available: https://valor.globo.com/patrocinado/dino/noticia/2023/09/28/falhas-no-fornecimento-de-energia-prejudicam-industrias.ghtml

[3] D. O. Johnson and K. A. Hassan, "Issues of power quality in electrical systems," *Int. J. Energy Power Eng.*, vol. 5, no. 4, pp. 148–154, 2016, doi: 10.11648/j.ijepe.20160504.12.

[4] ANEEL, "Módulo 8 - Qualidade do fornecimento de energia elétrica," 2021. Accessed: Sep. 07, 2025 (in Portuguese). [Online]. Available: https://www.gov.br/aneel/pt-br/centrais-de-conteudos/procedimentos-regulatorios/prodist

[5] D. O. Anggriawan, E. Wahjono, I. Sudiharto, A. A. Firdaus, D. N. N. Putri, and A. Budikarso, "Identification of short duration voltage variations based on short time fourier transform and artificial neural network," in *Proc. 2020 Int. Electron. Symp.*, 2020, pp. 43–47, doi: 10.1109/IES50839.2020.9231815.

[6] F. R. Zaro, M. A. Abido, S. Ameenuddin, and I. M. Elamin, "Characterization of short-duration voltage events," in *Proc. 2012 IEEE Int. Conf. Power Energy*, 2012, pp. 650–654, doi: 10.1109/PECon.2012.6450294.

[7] G. R. d. Santos, N. C. d. Jesus, J. M. Machado, J. R. Cogo, W. S. d. Jesus, and T. P. Franco, "Análise dos impactos associados às ocorrências de variações de tensão de curta duração na operação de uma planta industrial de papel e celulose," in *Proc. 2023 XV Braz. Conf. Qual. Power*, 2023, pp. 1–6, doi: 10.1109/CBQEE59548.2023.10503696.

[8] F. B. Bottura and M. Oleskovicz, "Optimal allocation of power quality monitors considering short-duration voltage variations and parallel harmonic resonance conditions in power distribution systems," *Int. J. Elect. Power Energy Syst.*, vol. 144, 2023, Art. no. 108580, doi: 10.1016/j.ijepes.2022.108580.

[9] A. R. Ferreira, B. M. Gianesini, J. C. Oliveira, and P. H. O. Rezende, "An approach for assigning responsibilities of short-term voltage variations in electrical power systems," *IEEE Access*, vol. 11, pp. 7751–7758, 2023, doi: 10.1109/ACCESS.2023.3237921.

[10] QGIS Team Development, "QGIS," 2025. Accessed: Apr. 07, 2025. [Online]. Available: https://qgis.org/project/overview/

[11] A. G. d. Souza and W. M. S. Bernardes, "bdgd2dss: Ferramenta para modelagem de alimentadores da BDGD para uso com OpenDSS," (in Portuguese), 2025. Accessed: Sep. 07, 2025. [Online]. Available: https://pypi.org/project/bdgd2dss/

[12] P. Radatz and Contributors, "bdgd2opendss: A BDGD to OpenDSS conversion tool," 2024. Accessed: Apr. 4, 2025. [Online]. Available: https://github.com/pauloradatz/bdgd2opendss

[13] D. Montenegro, M. Hernandez, and G. A. Ramos, "Real time OpenDSS framework for distribution systems simulation and analysis," in *Proc. 2012 6th IEEE/PES Transmiss. Distribution: Latin Amer. Conf. Expo.*, 2012, pp. 1–5, doi: 10.1109/TDC-LA.2012.6319069.

[14] R. B. Roy, S. Alahakoon, P. J. V. Rensburg, and S. J. Arachchillage, "Impact analysis of uncoordinated electric ferry charging on distribution network," in *Proc. Adv. Elect. Eng., Electron. Energy*, 2024, vol. 10, doi: 10.1016/j.prime.2024.100783, Art. no. 100783.

[15] R. F. Espinoza and P. Godoy, "Opendss-based real-time RMS simulator: Design and applications," in *Proc. 2024 Open Source Modelling Simul. Energy Syst.*, 2024, pp. 1–7, doi: 10.1109/OSMSES62085.2024.10668999.

[16] R. S. Bonadia, F. C. L. Trindade, W. Freitas, and B. Venkatesh, "On the potential of ChatGPT to generate distribution systems for load flow studies using OpenDSS," *IEEE Trans. Power Syst.*, vol. 38, no. 6, pp. 5965–5968, Nov. 2023, doi: 10.1109/TPWRS.2023.3315543.

[17] T. Pham, T. Nguyen, and L. Kien, "Optimal placement of photovoltaic distributed generation units in radial unbalanced distribution systems using MATLAB and OpenDSS-based co-simulation and a proposed meta-heuristic algorithm," *Int. Trans. Elect. Energy Syst.*, vol. 2022, 2022, Art. no. 1446479, doi: 10.1155/2022/1446479.

[18] M. Toledo-Orozco, E. Bravo-Padilla, C. Álvarez, D. B. Morales-Jadan, and L. Gonzalez-Morales, "Methodological evaluation to integrate charging stations for electric vehicles in a tram system using OpenDSS: A case study in Ecuador," *Sustainability*, vol. 15, no. 8, 2023, Art. no. 6382, doi: 10.3390/su15086382.

[19] P. Radatz, "Py-dss-interface," 2023. Accessed: Apr. 04, 2025. [Online]. Available: https://pypi.org/project/py-dss-interface/

[20] E d. O. Monteiro and A. L. F. Filho, "Comparative analysis of regulatory procedures for classifiying short-duration voltage variations," in *Proc. 17th Int. Conf. Harmon. Qual. Power*, 2016, pp. 569–574, doi: 10.1109/ICHQP.2016.7783308.

[21] H. Zhang, G. Xiao, and Z. Lu, "Fast detection of short-duration grid voltage RMS variation for compensation applications," in *Proc. 2021 IEEE 12th Energy Convers. Congr. Expo. - Asia*, 2021, pp. 833–838, doi: 10.1109/ECCE-Asia49820.2021.9479387.

[22] A. Fioravanti, A. Prudenzi, E. Fiorucci, A. Silvestri, and S. Mari, "The effect of short duration voltage sags on LED lamps," in *Proc. 2024 Int. Symp. Power Electron., Elect. Drives, Automat. Motion*, 2024, pp. 436–441, doi: 10.1109/SPEEDAM61530.2024.10609106.

[23] L. A. d. Costa, D. d. S. Gazzana, and R. C. Leborgne, "Fuzzy logic applied to impact assessment of short-duration RMS voltage variation," in *Proc. 54th Int. Universities Power Eng. Conf.*, 2019, pp. 1–6.

[24] M. Priyadarshini and M. Sushama, "Classification of short-duration voltage variations using wavelet decomposition based entropy criteria," in *Proc. 2016 Int. Conf. Wireless Commun., Signal Process. Netw.*, 2016, pp. 2192–2196.

[25] M. S. Priyadarshini, D. Krishna, M. B. Reddy, A. Bhatt, M. Bajaj, and M. M. Mahmoud, "Continuous wavelet transform based visualization of transient and short duration voltage variations," in *Proc. 4th IEEE Glob. Conf. Advance. Technol.*, 2023, pp. 1–6.

[26] P. R. Kamthekar, P. V. Gautam, and R. K. Munje, "Detection, characterization and classification of short duration voltage events using DWT and fuzzy logic," in *Proc. 2017 Int. Conf. Innov. Mechanisms Ind. Appl.*, 2017, pp. 242–247.

[27] D. K. Filiu and J. C. Cebrian, "A novel stochastic methodology to estimate the impact factor due to short-duration voltage variations in power distribution networks," *Electric Power Syst. Res.*, vol. 247, 2025, Art. no. 111773. [Online]. Available: https://www.sciencedirect.com/science/article/pii/S0378779625003657

[28] V. Liubčuk, G. Kairaitis, V. Radziukynas, and D. Naujokaitis, "IIR shelving filter, support vector machine and k-nearest neighbors algorithm application for voltage transients and short-duration RMS variations analysis," *Inventions*, vol. 9, no. 1, 2024, Art. no. 12. [Online]. Available: https://www.mdpi.com/2411-5134/9/1/12

[29] L. A. d. Costa, Y. Mohammadi, R. C. Leborgne, and D. d. S. Gazzana, "Impact evaluation of the neutral-grounding resistance on short-duration RMS voltage variations," in *Proc. 19th Int. Conf. Harmon. Qual. Power*, 2020, pp. 1–6.

[30] C. Yuan et al., "A critical load voltage regulator with both voltage sag compensation and fluctuation mitigation functions," *Int. J. Elect. Power Energy Syst.*, vol. 170, 2025, Art. no. 110870. [Online]. Available: https://www.sciencedirect.com/science/article/pii/S0142061525004181

[31] V. A. Skolota and G. S. Zinovev, "Detecting voltage swell, interruption and sag," in *Proc. 19th Int. Conf. Young Specialists Micro/Nanotechnologies Electron Devices*, 2018, pp. 6403–6408, doi: 10.1109/EDM.2018.8434940.

[32] M. Paolone et al., "Fundamentals of power systems modelling in the presence of converter-interfaced generation," *Electric Power Syst. Res.*, vol. 189, 2020, Art. no. 106811, doi: 10.1016/j.epsr.2020.106811.

[33] C. M. Furse, M. Kafal, R. Razzaghi, and Y.-J. Shin, "Fault diagnosis for electrical systems and power networks: A review," *IEEE Sensors J.*, vol. 21, no. 2, pp. 888–906, Jan. 2021, doi: 10.1109/JSEN.2020.2987321.

[34] U. A. Bordalo, A. B. Rodrigues, and M. G. Silva, "A new methodology for probabilistic short-circuit evaluation with applications in power quality analysis," *IEEE Trans. Power Syst.*, vol. 21, no. 2, pp. 474–479, May 2006, doi: 10.1109/TPWRS.2006.873055.

[35] D. B. Martins, "Probabilistic short-circuit analysis in power distribution systems with distributed generation," Master in Electrical Engineering (Dissertation), São Carlos School Eng., Univ. São Paulo, São Carlos, Brazil, (in Portuguese), 2021, doi: 10.11606/D.18.2021.tde-24032021-102152.

[36] V. Kumar, P. Jeyanthy, K. Mahesh, P. Akila, V. S. Thrisha, and B. M. Swetha, "Fault classification & detection in IEEE 34 bus system using convolutional neural network," in *Proc. 15th Int. Conf. Comput. Commun. Netw. Technol.*, 2024, pp. 1–6, doi: 10.1109/ICCCNT61001.2024.10725909.

[37] W. L. Rodrigues Jr, D. M. Reis, F. A. S. Borges, F. H. D. Araújo, A. O. d. C. Filho, and R. d. A. L. Rabelo, "Localization of voltage SAG sources using convolutional neural network in IEEE 34-bus system," in *Proc. 2020 IEEE Int. Conf. Syst., Man, Cybern.*, 2020, pp. 2836–2841, doi: 10.1109/SMC42975.2020.9283083.

[38] I. R. A. Rodrigues and A. d. Conti, "Protection study of a microgrid based on the 34-Bus IEEE distribution feeder," in *Proc. 2018 Simpósio Brasileiro de Sistemas Eletricos*, 2018, pp. 1–6, doi: 10.1109/SBSE.2018.8395588.

[39] R. C. Dugan and W. H. Kersting, "Induction machine test case for the 34-bus test feeder - description," in *Proc. 2006 IEEE Power Eng. Soc. Gen. Meeting*, 2006, pp. 1–4, doi: 10.1109/PES.2006.1709506.

[40] Google, "Google Earth," 2025. Accessed: Apr. 04, 2025. [Online]. Available: https://www.google.com/earth/

[41] ANEEL, "CEMIG-D 4950 2022-12-31," 2022. Accessed: Apr. 04, 2025. [Online]. Available: https://dadosabertos-aneel.opendata.arcgis.com/search?collection=Dataset

[42] ANEEL, "PRODIST - Procedimentos de distribuição de energia elétrica no sistema elétrico nacional," 2022. Accessed: Sep. 06, 2025 (in Portuguese). [Online]. Available: https://www.gov.br/aneel/pt-br/centrais-de-conteudos/procedimentos-regulatorios/prodist

[43] A. G. d. Souza, "Attribution-SDVV-feeders," GitHub Repository, 2025. Accessed: Aug. 31, 2025. [Online]. Available: https://github.com/ArthurGS97/Attribution-SDVV-feeders

[44] ANEEL, "Module 7 - Calculation of distribution losses," 2022. Accessed: Sep. 02, 2025 (in Portuguese). [Online]. Available: https://www2.aneel.gov.br/cedoc/aren2021956_2_6.pdf

[45] ANEEL, "Module 10 - Regulatory geographic information system," 2022. Accessed: Apr. 04, 2025 (in Portuguese). [Online]. Available: https://www2.aneel.gov.br/cedoc/aren2021956_2_9.pdf

[46] ANEEL, "Technical Report n. 0057/2014-SRD/ANEEL," 2014. Accessed: Apr. 04, 2025 (in Portuguese). [Online]. Available: https://www2.aneel.gov.br/aplicacoes/audiencia/arquivo/2014/026/documento/nota_tecnica_0057_srd.pdf

[47] Python Software Foundation, "Python-TM," 2025. Accessed: Apr. 20, 2025. [Online]. Available: https://www.python.org/

[48] W. McKinney, "Data structures for statistical computing in python," in *Proc. 9th Python Sci. Conf.*, S. van der Walt and J. Millman, Eds., Austin, TX, USA, 2010, pp. 56–61, doi: 10.25080/Majora-92bf1922-00a.

[49] J. D. Hunter, "Matplotlib: A 2D graphics environment," *Comput. Sci. Eng.*, vol. 9, no. 3, pp. 90–95, 2007, doi: 10.1109/MCSE.2007.55.

[50] EPRI, "OpenDSS manual," 2020. Accessed: Apr. 04, 2025. [Online]. Available: https://www.epri.com/pages/sa/opendss

[51] A. L. S. Pessoa and M. Oleskovicz, "Fault location algorithm for distribution systems with distributed generation based on impedance and metaheuristic methods," *Electric Power Syst. Res.*, vol. 225, 2023, Art. no. 109871, doi: 10.1016/j.epsr.2023.109871. [Online]. Available: https://www.sciencedirect.com/science/article/pii/S0378779623007599?via\%3Dihub

[52] A. P. Mazzini, W. M. S. Bernardes, F. M. d. Vasconcelos, F. d. O. Saraiva, and E. N. Asada, "Application of artificial neural networks for discrimination of nonlinear loads," in *Proc. 2013 IEEE PES Conf. Innov. Smart Grid Technol. (ISGT Latin Amer.)*, 2013, pp. 1–7, doi: 10.1109/ISGT-LA.2013.6554422.

[53] F. M. Vasconcelos et al., "Artificial neural network applied to prediction of electricity generated by grid connected photovoltaic systems," in *Proc. 2013 IEEE PES Conf. Innov. Smart Grid Technol. (ISGT Latin Amer.)*, 2013, pp. 1–6, doi: 10.1109/ISGT-LA.2013.6554453.

[54] F. O. Saraiva, W. M. S. Bernardes, and E. N. Asada, "A framework for classification of non-linear loads in smart grids using artificial neural networks and multi-agent systems," *Neurocomputing*, vol. 170, pp. 328–338, 2015, doi: 10.1016/j.neucom.2015.02.090. [Online]. Available: https://www.sciencedirect.com/science/article/abs/pii/S0925231215009285

[55] W. M. S. Bernardes and F. M. Vasconcelos, "Forecasting electric power generation of grid-connected solar photovoltaic systems by using artificial neural networks," in *Proc. Simpósio Brasileiro de Automação Inteligente*, 2019, pp. 1–8, doi: 10.17648/sbai-2019-111138, (in Portuguese). [Online]. Available: https://proceedings.science/p/111138

[56] B. Masalmeh, R. Prasad, V. Nougain, and A. Lekić, "Neural networks in RSCAD: Enhancing MMC-based HVDC simulation with advanced machine learning," *IEEE Trans. Ind. Appl.*, vol. 61, no. 2, pp. 2515–2526, Mar./Apr. 2025, doi: 10.1109/TIA.2025.3529804.

[57] W. Lin, F. Li, Q. Ran, and Z. Yang, "Training a trustworthy DNN for optimal power flow in active distribution networks," *IEEE Trans. Ind. Appl.*, vol. 61, no. 1, pp. 1716–1724, Jan./Feb. 2025, doi: 10.1109/TIA.2024.3430270.

[58] U. Qureshi et al., "Optimizing electric vehicle integration in virtual power plants: A stochastic optimization framework with MDNN integration," *IEEE Trans. Ind. Appl.*, vol. 60, no. 6, pp. 9227–9236, Nov./Dec. 2024, doi: 10.1109/TIA.2024.3444744.

Arthur Gomes de Souza was born in Correntina, Bahia, Brazil. He received the bachelor's degree in electrical engineering and the M.Sc. degree in electrical engineering with a focus on power system protection from the Federal University of Uberlândia, Uberlândia, Brazil, in 2021, He is currently working toward the Ph.D. degree. His graduate studies are financially supported by Coordination for the Improvement of Higher Education Personnel. As a Researcher with the Laboratory of Alternative Energies and Power System Protection, he has worked on a range of topics, including feeder modeling and simulation, and the optimization of protection systems in electrical networks. He is proficient in tools such as *OpenDSS*, *Python*™ and *QGIS*, with several publications demonstrating his expertise in these areas. His research interests include electrical system modeling, protection coordination, and the application of advanced optimization techniques—such as evolutionary algorithms for coordinating protective devices in distribution networks.

Luiz Arthur Tarralo Passatuto was born in Colina, São Paulo, Brazil. He received the B.Sc. and M.Sc. degrees in electrical engineering in 2021 and 2025, respectively, from the Federal University of Uberlândia, Uberlândia, Brazil,, where he is currently working toward the Ph.D. degree. As a Researcher with the Laboratory of Alternative Energies and Power System Protection, he has worked with optimization in electric power system protection using metaheuristics, developing software tools that use Blockchain and power system modeling with distributed energy resources. He has good knowledge in programming with *Python*™ and *OpenDSS* tool. His research interests include power system analysis, protection studies, solving engineering problems with optimization techniques, and incorporation of distributed energy resources in the electrical network.

Wellington Maycon Santos Bernardes was born in Goiânia - Goiás, Brazil. He received the B.Sc. degree in electrical engineering from Federal University of Uberlândia (*UFU*), Uberlândia, Brazil, in 2010, and the M.Sc. and Ph.D. degrees in electrical engineering from São Carlos School of Engineering, University of São Paulo, São Paulo, Brazil, in 2013 and 2018, respectively. He has undertaken a mobility period (Sandwich Ph.D.) supported by the prestigious scholarship of the European Commission's Erasmus Mundus Programme with the Faculty of Engineering, University of Porto, Porto, Portugal. He was a Professor with *UFU* in 2019, a Coordinator with the Laboratory of Alternative Energies and Power System Protection, an *ad hoc* Consultant for the State Funding Agency of Distrito Federal, and the National Institute of Educational Studies and Research Anísio Teixeira, Brasília - DF. Extensive experience in academic administration, serving as Coordinator with the Department of Electric Power Systems, and a Undergraduate Coordinator of the Electrical Engineering Program. He also has expertise in power systems projects, funded by Brazilian research foundations (*CNPq*, *CAPES*, *FAPEMIG*, *FAPESP*) and utility companies. His research interests include power system protection, alternative energies, measurement and uncertainty analysis, optimization and applications of artificial intelligence in electrical networks, energy efficiency, and power quality.

Luiz Carlos Gomes Freitas was born in Uberlândia, Brazil, in 1976. He received an undergraduate degree in electrical engineering with emphasis on power systems, and the M.Sc. and Ph.D. degrees in electrical engineering with emphasis on power electronics from the Federal University of Uberlândia (*UFU*), Uberlândia, Brazil, in 2001, 2003, and 2006, respectively. In his doctoral thesis, he developed an innovative topological design of a three-phase hybrid rectifier for high power drive systems. In 2008, he joined as the Faculty Member with the *UFU*, where he is developing teaching and research activities in the area of power electronics and power systems. Since 2010, he is the Coordinator of the Power Electronics Research Center, Faculty of Electrical Engineering, *UFU*. His research interests include electrical engineering, conversion and rectification of electric energy, working on various topics related to power electronics, electric power quality, and renewable energy. In 2012, he was th recipient of the Second Prize Paper Award of the IEEE-IAS-Industrial Automation and Control Committee for his contribution to the development of hybrid rectifier structures. Since 2013, he is a Researcher recognized by the National Council for Scientific and Technological Development (*CNPq*) with a Research Productivity Grant.

Ênio Costa Resende received the bachelor's degree in electrical engineering from the Federal University of Uberlândia (*UFU*), Uberlândia, Brazil, including an exchange period through the *CsF / CAPES* Program with Sacramento State University (SAC-State), Sacramento, CA, USA, in 2018, the M.Sc. degree in electrical engineering with a specialization in power electronics from Power Electronics Research Center, *UFU,* Postgraduate Program, in 2020, and the Ph.D. degree in electrical engineering in 2024. During his doctoral studies, he was a Visiting Researcher with the University of Vaasa, Vaasa, Finland, from 2023 to 2024, where he worked on Neural Networks and Fuzzy Logic, focusing on islanding detection techniques, synchronization strategies, and maximum power point tracking (MPPT) methods. He is currently a Postdoctoral Researcher with *UFU*, working on hybrid microgrids, battery charging systems, and electric vehicle charging stations. His research interests include islanding detection, distributed generation, renewable energies, MPPT, control methods, power quality, microgrids, embedded control, and dual-active-bridge converters.